RSC Publishing Faraday Discussions

Hierarchically Patterned Striped Phases of Polymerized Lipids: Toward Controlled Carbohydrate Presentation at Interfaces

Journal:	*Faraday Discussions*
Manuscript ID	FD-ART-02-2019-000022.R1
Article Type:	Paper
Date Submitted by the Author:	05-Mar-2019
Complete List of Authors:	Davis, Tyson; Purdue University, Chemistry Bechtold, Jeremiah; Purdue University, Chemistry Hayes, Tyler; Purdue University, Chemistry Villarreal, Terry; Purdue University, Chemistry Claridge, Shelley; Purdue University, Chemistry and Biomedical Engineering

ARTICLE

Hierarchically Patterned Striped Phases of Polymerized Lipids: Toward Controlled Carbohydrate Presentation at Interfaces

Received 00th January 20xx,
Accepted 00th January 20xx

DOI: 10.1039/x0xx00000x

Tyson C. Davis,[a,c] Jeremiah O. Bechtold, [a,c] Tyler R. Hayes,[a] Terry A. Villarreal[a] and Shelley A. Claridge [a,b]

Complex biomolecules, including carbohydrates, frequently have molecular surface footprints larger than those in broadly utilized standing phase alkanethiol self-assembled monolayers, yet would benefit from structured orientation and clustering interactions promoted by ordered monolayer lattices. Striped phase monolayers, in which alkyl chains extend across the substrate, have larger, more complex lattices: nm-wide stripes of headgroups with 0.5 or 1-nm lateral periodicity along the row, separated by wider (~5 nm) stripes of exposed alkyl chains. These anisotropic interfacial patterns provide a potential route to controlled clustering of complex functional groups such as carbohydrates. Although the monolayers are not covalently bound to the substrate, assembly of functional alkanes containing an internal diyne allows such monolayers to be photopolymerized, increasing robustness. Here, we demonstrate that, with appropriate modifications, microcontact printing can be used to generate well-defined microscopic areas of striped phases of both single-chain and dual-chain amphiphiles (phospholipids), including one (phosphoinositol) with a carbohydrate in the headgroup. This approach generates hierarchical molecular-scale and microscale interfacial clustering of functional ligands, prototyping a strategy of potential relevance for glycobiology.

Introduction

Interfaces with precisely constructed chemical environments at micrometer and nanometer scales are required for applications ranging from the design of electronic devices to the controlled display of complex biomolecules.[1] Increasingly, the goals of controlling interfacial structure may include not only positioning functional groups on the surface, but also controlling their orientation, clustering, or placement relative to other functional groups, mimicking complex structures such as those in cell membranes.

Monolayers of molecules such as alkanethiols have been broadly utilized to structure interfacial chemistry, particularly on coinage metals.[2] In alkanethiol monolayers, ordered lattices of alkyl chains position terminal functional groups with nearest-neighbor distances ~0.5 nm, tilted at angles influenced by the bond between the thiol and the substrate.[2] Lattices displaying simple functional groups (*e.g.* carboxylic acids) influence further assembly at the interface (*e.g.* selecting for specific crystal facets of calcite); microcontact printing enables geometrically patterned assembly over microscopic (or large nanoscopic) areas.[3-5]

Controlling presentation of more complex, biologically relevant functionalities raises new challenges. In biological environments, polysaccharides, peptides, and other entities are presented in controlled orientations, with both nanoscale and microscale spatial ordering. To mimic elements of these environments for applications such as high-throughput screening of biomolecular interactions,[6-7] it would be useful to present microstructured areas of surface containing nanostructured clusters of specific ligand chemistries, enabling multivalent binding similar to molecular recognition events in the glycocalyx.[8-17]

However, even monosaccharides occupy interfacial footprints substantially greater than that of an alkyl chain in an alkanethiol monolayer (~0.25 nm^2). Thus, creating simple lattices of these larger moieties becomes less straightforward. Designing complex clusters of functional groups at biologically relevant scales—with linear dimensions large relative to alkyl chain nearest neighbor distances in standing phases (>0.5 nm) but small relative to those typically achieved through microcontact printing (significantly < 100 nm)—becomes especially challenging.

One complementary strategy for clustering structures with larger footprints arises from a transformation to the monolayer structure.[1] Since at least the 1960s, it has been known that long-chain alkanes can adopt lying down orientations on graphite and other layered materials such as MoS_2 and WS_2.[18-19] More recently, the surface chemistry of 2D materials (particularly graphite and graphene) has been regulated using striped phases of functional alkanes,[18-23] in which the alkyl chains extend horizontally across the substrate. Scanning probe microscopy studies[18-23] have shown that this arrangement produces nm-wide stripes of headgroups with 0.5 or 1-nm lateral periodicity along the row (for single-chain and dual-chain amphiphiles, respectively), separated by wider (~5 nm, dependent

[a] *Department of Chemistry, Purdue University, West Lafayette, IN 47907.*
[b] *Weldon School of Biomedical Engineering, Purdue University, West Lafayette, IN 47907.*
[c] *These two authors made equal contributions.*
Electronic Supplementary Information (ESI) available: detailed experimental methods, large-scale SEM images. See DOI: 10.1039/x0xx00000x

on chain length) stripes of exposed alkyl chains. Assembly of functional alkanes containing an internal diyne allows the monolayer to be photopolymerized, creating a conjugated ene-yne polymer backbone that has been studied extensively in the context of molecular electronics.[21,23-24] Polymerization also stabilizes the noncovalently adsorbed monolayer, increasing potential utility of patterns of functional groups displayed at the interface.[25-27]

Just as clustering of functional groups at biological active sites creates unique chemical environments to promote specific interactions, precise positioning of functional groups in striped phases also creates unique chemical environments (Fig. 1). We have observed that striped phases of diyne phospholipids[26] exhibit distinct characteristics in comparison with striped phases composed of other amphiphiles.[28] Phospholipids can adopt a 'sitting' orientation in which the terminal amine in the headgroup protrudes a few Ångströms from the interface.[26] The phosphate and ester functional groups create a tailored chemical environment around the amine. Both head and chain structures influence nano- and micro-scale assembly of striped phases,[27,29-30] and chain elements including the position of the polymer backbone can be used to modulate solvent availability of the polar headgroups.[28] Flexible 1D zwitterionic arrays formed by the striped phase also impact further assembly of inorganic and organic nanostructures at the interface.[31-32] More broadly, the striped phospholipid polymer architecture represents a potential means for flexible yet controlled presentation of ligands at the interface.

Microcontact printing of striped phases (Fig. 1d) has the potential to combine microscopic geometric control over surface chemistry with molecular-scale control over ligand presentation, a capability of potential use in glycobiology. However, the strong focus on molecular-scale structure in noncovalent striped-phase monolayers on highly oriented pyrolytic graphite (HOPG) has meant that such monolayers are typically ordered and characterized at length scales <100 nm.[33-35] Recently, we have shown that some amphiphiles order into striped phases with edge lengths >10 μm,[27] scales relevant to controlling interactions with biological entities, and that monolayer ordering can be characterized by scanning electron microscopy (SEM), making it possible to characterize surface functionalization up to mm scales.[29-30,36] Some noncovalent monolayers can also be robust enough to survive vigorous solution processing and other environmental interactions.[27,31]

Here, we demonstrate microcontact printing of striped phases of amphiphiles on HOPG, utilizing both diyne amphiphiles (*e.g.* diynoic acids, diyne phospholipids) and a saturated phosphoinositol. This approach generates hierarchical molecular-scale and microscale interfacial clustering of functional ligands, including carbohydrates, prototyping a strategy of potential relevance for controlled presentation of carbohydrates at interfaces.

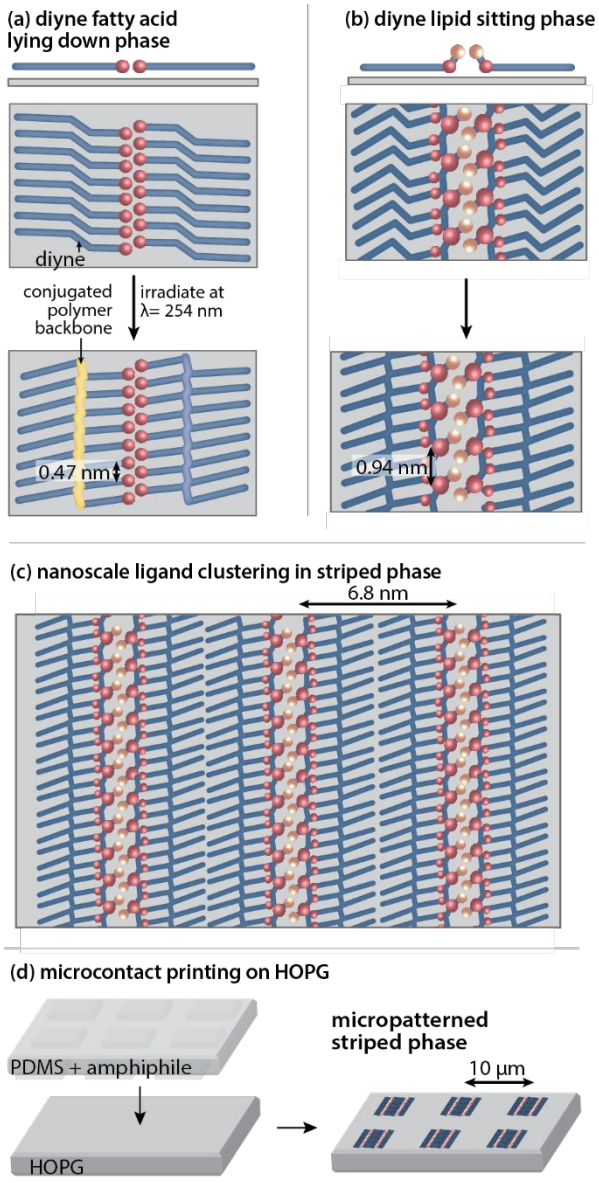

Fig. 1. Illustrations of: (a) striped phase of diynoic acids on HOPG, showing 0.47 nm distance between functional groups along stripe direction; (b) striped phase of diyne phospholipids, showing 0.94 nm distance between functional groups along row; (c) multiple rows of striped phase, showing lamellar periodicity, a route to nanoscale ordering of complex functional groups; and (d) illustration of poly(dimethylsiloxane) (PDMS) transfer of amphiphiles to HOPG to form striped phases.

Results and Discussion

Preparation of striped monolayers on HOPG. Striped monolayers of both single-chain amphiphiles (*e.g.* 10,12-pentacosadiynoic acid (PCDA), Figure 2a,b) and dual-chain amphiphiles (*e.g.* 1,2-bis(10,12-tricosadiynoyl)-*sn*-glycero-3-phosphocholine (diyne PC), Figure 2a,c) are typically prepared via drop-casting or Langmuir-Schaefer (LS) conversion,[23,26-27,31,37-38] then polymerized via UV irradiation and characterized by atomic force microscopy (AFM) (Figure 2d,e). In AFM images, striped lamellar patterns are oriented at 120° angles, in epitaxy with the HOPG lattice; each stripe represents a row of lying-

down molecules. SEM images of striped phases (Fig. 2f–i) typically exhibit brighter areas representing the molecular domains, against a darker background of HOPG. Long linear features along the image diagonals in Fig. 2f,g represent step edges in the HOPG substrates. Higher-resolution SEM images (Fig. 2h,i) reveal linear defects within the ordered molecular domains, highlighting the directionality of the molecular rows.[29] Use of this combination of techniques enables us to characterize both microscopic and nanoscopic ordering in striped phases, including those with carbohydrate headgroups (*vide infra*).

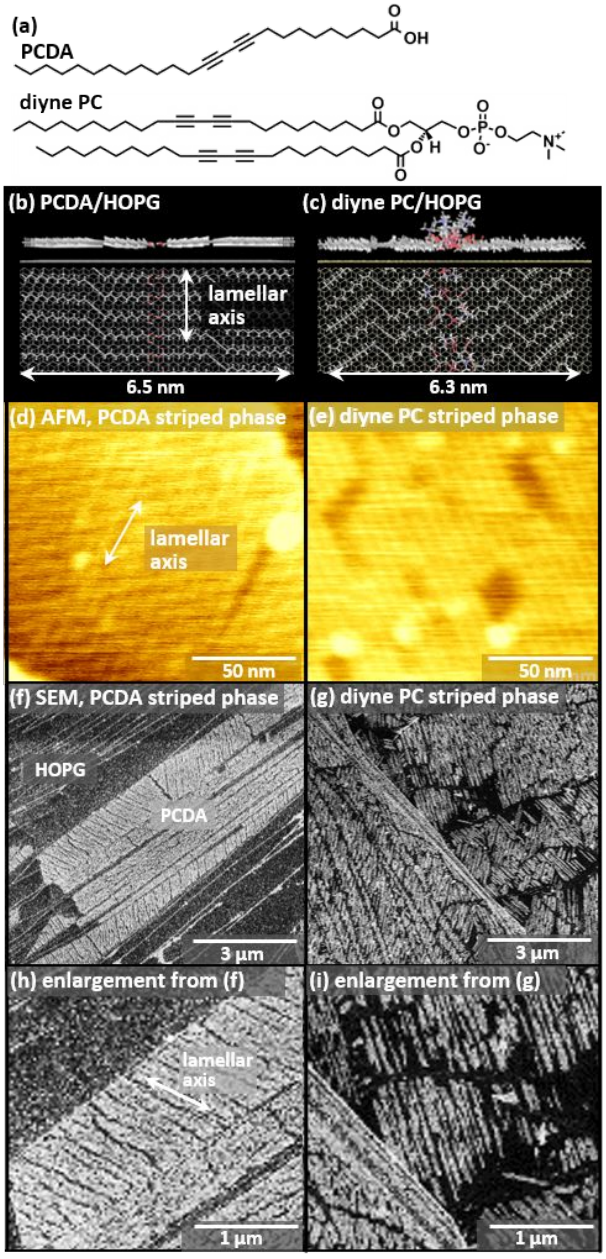

Fig 2. (a) Structures of PCDA and diyne PC. (b,c) Molecular models of striped phases of (b) PCDA and (c) diyne PC on HOPG. (d,e) AFM images of striped phases of (d) PCDA and (e) diyne PC, illustrating lamellar pattern. (f–i) SEM images of striped phases of (f,h) PCDA and (g,i) diyne PC, illustrating long-range ordering.

Preparation of patterned striped monolayers on HOPG by microcontact printing. Microscopic patterns of striped phase monolayers were prepared on HOPG by microcontact printing,[14] as shown in Fig. 3. Stamps used for microcontact printing of alkanethiols on gold are commonly prepared with a 10:1 ratio of elastomer base to crosslinker, resulting in a nominal elastic modulus of ~2.6±0.02 MPa at commonly used curing conditions (65 °C, 1 h).[39] For transfer to HOPG, which has relatively low local surface roughness, we often found that stamps prepared with a 10:2 ratio of base to crosslinker (nominal elastic modulus 3.6±0.1 MPa)[39] improved transfer fidelity, while still enabling conformal contact.

A number of studies have previously examined factors relating to ink delivery to the substrate, with the goals of limiting diffusion of the ink outside the stamp contact area,[40-42] and limiting delivery of impurities from the PDMS stamp.[41,43] Delivering a controlled amount of diyne amphiphile to the substrate is especially important in assembling noncovalent monolayers; screening several possible methods for controlling diyne amphiphile delivery, we found that immersing the stamp in a solution of amphiphile in carrier solvent (1.1 mM for PCDA and single-chain amphiphiles, 0.55 mM for diyne PC and dual chain amphiphiles, maintaining the concentration of alkyl chains) generally maximized coverage of striped phase inside the contact area while minimizing coverage outside the contact area.

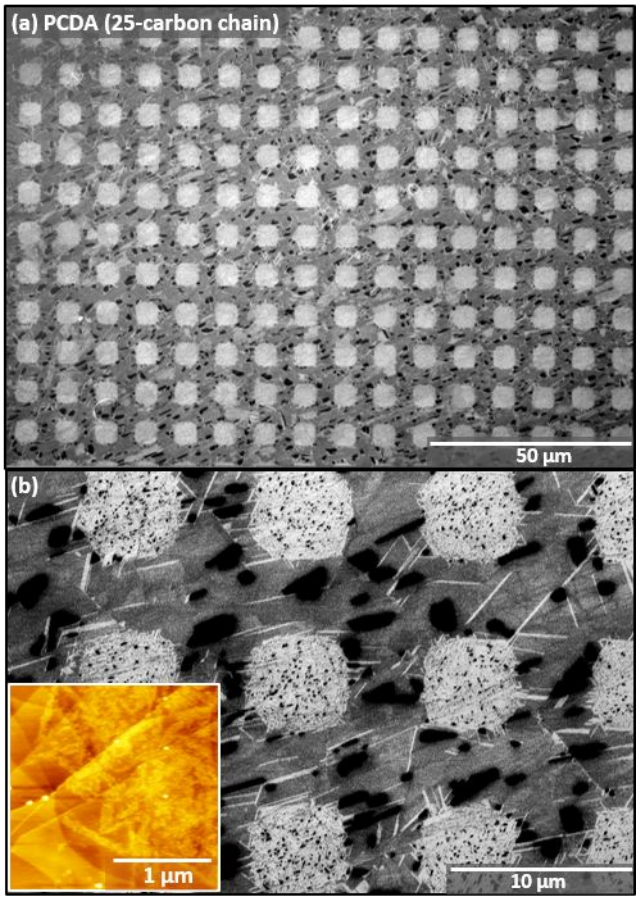

Fig 3. (a) SEM image of microscopic areas of PCDA striped phases assembled on HOPG by microcontact printing. (b) Higher-resolution SEM image illustrating coverage in square interior and small fractional coverage of molecular domains assembled outside stamp contact area. AFM image (inset in (b)) shows striped phase structure.

Ink concentrations used here are similar to those typically utilized for assembly of standing phases of alkanethiols on Au (1–10 mM),[2] although fewer molecules are required to fill a given area of the surface: the molecular footprint of an alkyl chain in a lying-down phase (1.5 nm^2 for PCDA) is much larger than for a standing phase (~0.25 nm^2). Fig. 3a and b show SEM images of a pattern of squares transferred to HOPG using the stamp preparation and inking conditions described above. Fig. 3b shows a higher-resolution image of the square pattern. High coverage is observed within the squares; AFM is used to verify that molecular coverage is comprised of striped domains (Fig. 3b, inset, and Supporting Information). Areas between the square stamp contact areas (channel regions) contain low number densities of long, narrow molecular domains characteristic of submonolayer island nucleation and growth under conditions of low surface monomer concentrations.[44] Areas between squares also contain material that appears in dark contrast in SEM images. Similar features appear on substrates brought into contact with stamps wetted with the carrier solvents in the absence of amphiphile (see Supporting Information). Deposition of impurities is also common in microcontact printing of alkanethiols on gold. Previous studies suggest that the deposited material is the oligomeric PDMS crosslinker, in which hydrosilyl groups undergo oxidation to form more polar species exhibiting increased solubility in the ink or carrier solvent.[43,45]

Transfer characteristics of single-chain amphiphiles based on chain length. In using a striped phase to pattern functionality at an interface, shorter chain lengths correspond to smaller stripe pitch values, and thus shorter distances between linear clusters of functional groups on the surface (Fig. 4a). However, chain length also impacts dynamics in the self-assembly process. In previous demonstrations of microcontact printing to form standing phases (e.g. alkanethiols on Au), others have observed that molecular diffusion around the stamp contact area increases for molecular inks with shorter chains.[46-48] Here, we tested transfer and assembly of 10,12-diynoic acids with chain lengths from 21 to 29 carbons to form noncovalently adsorbed striped phases to better understand the range of pitches that can reasonably be established, and the fidelity of patterning (Fig. 4b-d). In the figure, areas exhibiting linear defects typical of striped phases (similar to those in Fig. 2h) have been colored yellow as a guide to the eye. Image segmentation was used to estimate the average distance over which each amphiphile spread outside the stamped area in areas with good stamp contact (Fig. 4d, see Supporting Information for example AFM images used for segmentation). The average band through which molecules diffuse decreases in width from ~600 nm for HCDA to ~50 nm for NCDA. For all four carboxylic acids, the number density of domains is 10–20 per µm^2 within the contact area, which is reasonable given that the monomer concentration in the ink solution was the same for each molecule.

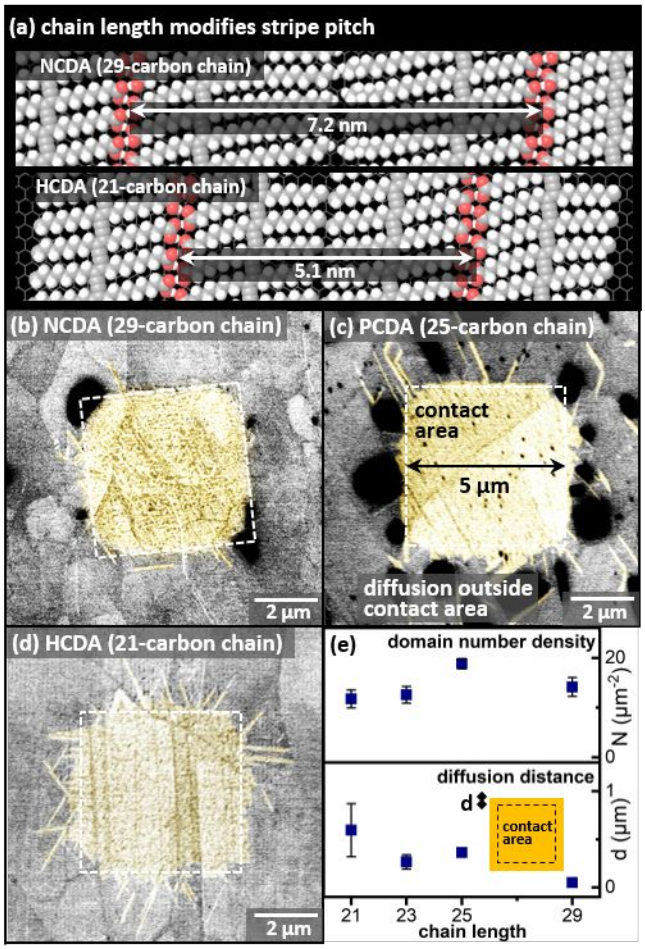

Fig 4. (a) Molecular models of diynoic acid striped phases with the longest (29 carbon) and shortest (21 carbon) chains utilized in these experiments. (b–d) SEM images of 10,12-diynoic acids: (b) nonacosadiynoic acid (NCDA, 29-carbon chain), (c) pentacosadiynoic acid (PCDA, 25-carbon chain), (d) henicosadiynoic acid (HCDA, 21-carbon chain). (e) Average domain number density per µm^2, N, and average distance molecular layer extends outside stamped area, d, for chain lengths from 21–29 carbons.

Transfer of dual-chain amphiphiles. Commercially available diyne phospholipids have two alkyl chains and a zwitterionic headgroup, which would be expected to modulate molecular transfer and spreading on the substrate in comparison with the single-chain carboxylic acids transferred above. Here, we test the transfer behavior of two diyne phospholipids, 23:2 diyne phosphocholine (diyne PC, Fig. 5) and 23:2 diyne phosphoethanolamine (diyne PE, Fig. 6). The phospholipid structures are identical with the exception that the bulky terminal quaternary ammonium in the PC headgroup (Fig. 5a) limits molecular packing in comparison with PE, which has a smaller terminal primary amine.

Transfer conditions similar to those optimized for single-chain amphiphiles result in a large fraction of standing phase formation (bright areas in square centers) (Fig. 5b, highlighted in yellow as a guide to the eye; also see Supporting Information). This is reasonable given the large number of alkyl carbons per molecule, promoting interchain interactions leading to standing phase formation. To mechanically destabilize interchain interactions (*e.g.* standing phases) on the stamp, and to initiate domain growth from a limited

area (to increase post-transfer molecular alignment), we tested molecular delivery by rolling the stamp along the HOPG surface (Fig. 5c,d, see Supporting Information for more experimental detail regarding rolling procedure). Testing transfer from stamps prepared with both 10:1 and 10:2 PDMS elastomer base:crosslinker ratios, we found that rolled contact increased the percentage of molecular transfer that produced striped phases (to near 100% for 10:2 stamps with rolled contact, Fig. 5e). Flat contact typically resulted in underfilling of the stamp contact area, while rolled contact resulted in average coverage zones extending nearly 1 μm outside the stamp contact area (as visible in Fig. 5d). In some cases (again, see Fig. 5d), rolled contact produced molecular alignment across the stamp contact areas (*i.e.*, lamellar axes aligned from upper left to lower right in Fig. 5d). Using other contact geometries, we have not observed this behavior, so with further optimization, rolled contact may represent a means of achieving long-range molecular alignment in printed striped phases, for applications in which such alignment is desirable.

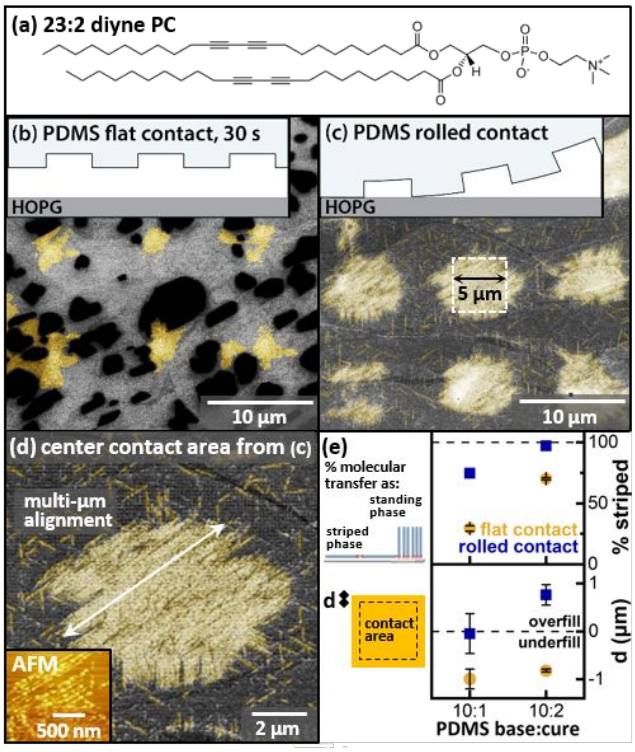

Fig. 5. (a) Structure of diyne PC. (b–d) SEM images of 0.5 mM diyne PC in EtOH transferred to HOPG using (b) 30 s flat contact and (c,d) rolled contact (stamp prepared at 10:2 base:crosslinker ratio). (e) Comparison of % striped phase (vs standing phase) molecular transfer with flat and rolled stamp contact, and fill of contact area, for PDMS stamps prepared with 10:1 and 10:2 base:crosslinker ratios.

Diyne PE (Fig. 6a) has a smaller terminal amine group that enables stronger lateral interactions between headgroups in standing phases, in comparison with the PC headgroup (which is bulky enough to limit packing). Importantly, the primary amine can also act as a functional handle for further coupling reactions, of potential utility in elaborating headgroups for glycobiological applications. Microcontact transfers of diyne PE in the conventional flat contact geometry also produced large areas of molecules assembled in standing phases (Fig. 6b). For transfer of diyne PE, the highest percentages of striped phase were observed for transfers in which the stamp surface hydrophilicity was increased by treatment with UV ozone plasma (a process which has been used previously to transfer hydrophilic molecules to create standing phase self-assembled monolayers (SAMs)). While multiple factors may contribute to the observed improvement in striped phase assembly during transfer, one possibility is that the hydrophilic stamp enables PE to assemble with polar headgroups oriented toward the stamp surface, with tails oriented favorably to mediate the initial stages of adsorption to HOPG for striped phase assembly. The differences in transfer behavior observed for molecules as structurally similar as diyne PE and diyne PC suggests a need to carefully balance molecule–stamp, molecule–molecule, and molecule–substrate interaction strengths for transfer of complex amphiphiles such as those relevant to glycobiology.

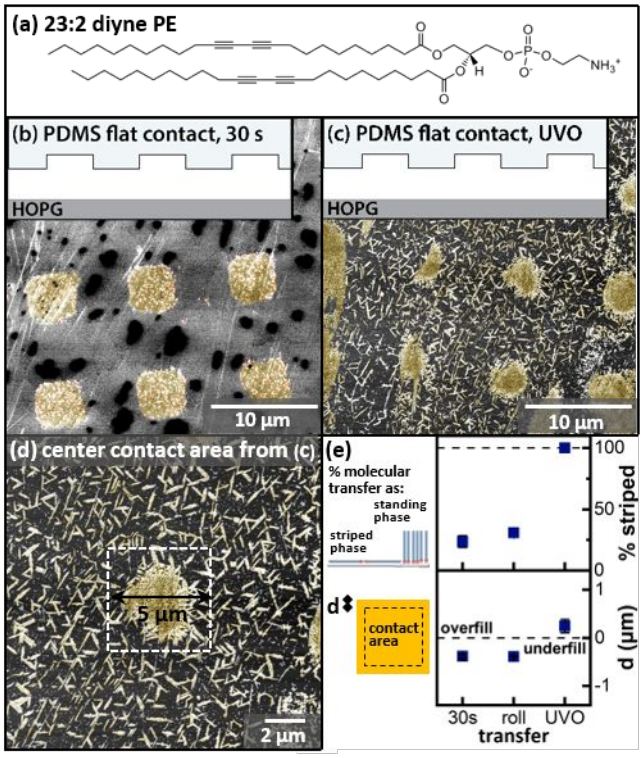

Fig 6. (a) Structure of diyne PE. (b–d) SEM images of 0.5 mM diyne PE in EtOH transferred to HOPG using (b) 30 s flat contact and (c,d) flat contact with stamp hydrophilicity increased with UV ozone (stamp prepared at 10:2 base:crosslinker ratio). (e) Comparison of % striped phase (vs standing phase) molecular transfer with flat contact, rolled contact, and flat contact with UV ozone, and fill of contact area, for PDMS stamps prepared with 10:2 base:crosslinker ratios.

Striped phases from carbohydrate-conjugated lipids. The procedures developed above are also useful for microcontact printing of phospholipids incorporating carbohydrates in the headgroups. Here, we demonstrate that 1,2-distearoyl-*sn*-glycero-3-phosphoinositol (18:0 PI, Fig. 7a), a phospholipid with an O-linked

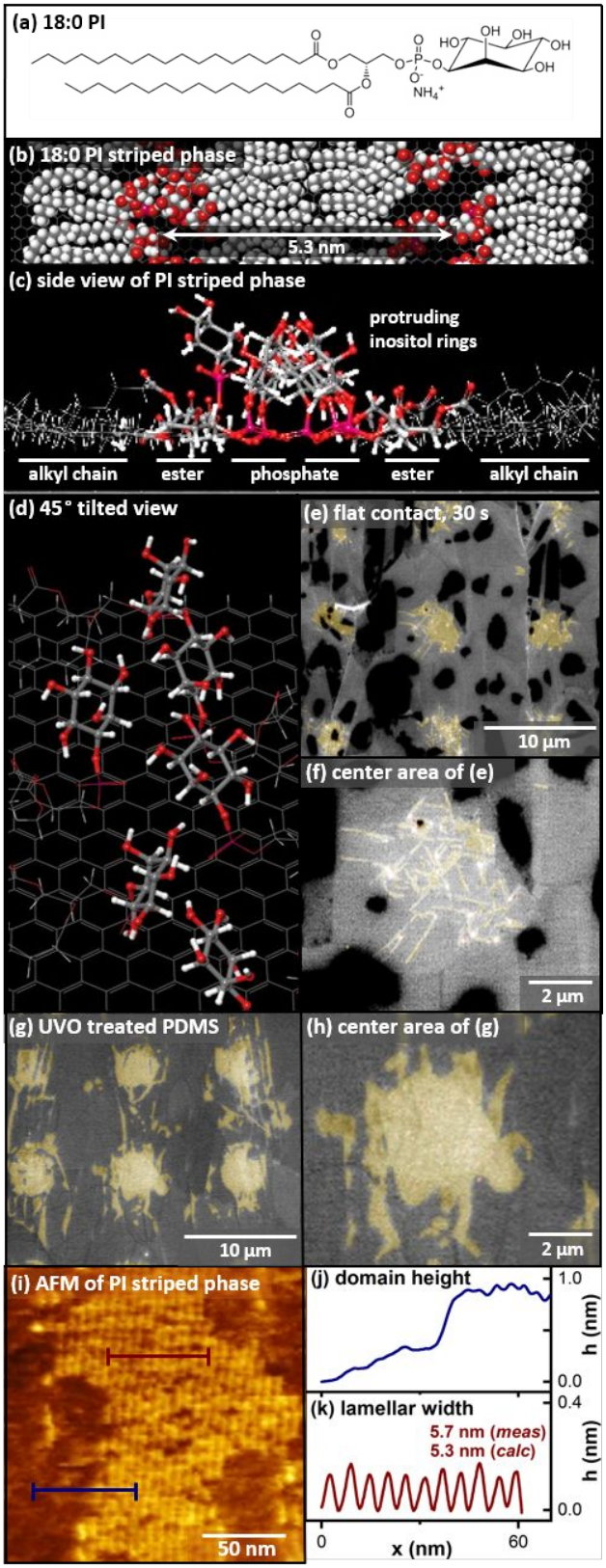

Fig 7. (a) Structure of 18:0 phosphoinositol (18:0 PI). (b–d) Minimized molecular models of striped phase of 18:0 PI on HOPG, illustrating: (b) lamellar width, (c) projection of inositol rings, in side view, (d) spacing of inositol rings (45 ° tilted view). (e–h) SEM images of PI striped phases formed using (e,f) rolling contact and (g,h) UV ozone-treated stamps for microcontact printing. (i) AFM image of PI striped phase, and line scans illustrating (j) domain height and (k) lamellar width.

monosaccharide appended to the phosphate, can assemble into striped phases through microcontact printing (Fig. 7b–d, models; Fig 7e–h, SEM). As with other phospholipids, bringing the stamp into flat contact with the HOPG substrate resulted in assembly of standing phases (see Supporting Information), while rolling contact or stamps treated with UV ozone produced striped phases with domain lengths in some cases >2 µm (Fig. 7f). Characterization of domain structure based on SEM images is more challenging for these amphiphiles, since they lack the polymerizable diyne group, and thus do not exhibit cracking defects under the electron beam. However, AFM images (Fig. 7i) reveal lamellar structure consistent with that predicted by molecular models, with average peak domain heights of ~0.8 nm (Fig. 7j, corresponding to inositol headgroup ridges), and measured lamellar widths of 5.7 nm (Fig. 7j), similar to the modeled values of 5.3 nm.

Conclusions

Here, we have demonstrated that it is feasible to use microcontact printing to create microscale striped patterns of amphiphiles. Stripes were printed using diynoic acids with chain lengths from 21–29 carbons, diyne phospholipids with phosphocholine and phosphoethanolamine headgroups, and phosphoinositol with 18-carbon saturated chains. The lamellar structures assembled in this way present 1-nm-wide stripes of functional headgroups with pitches from 5–10 nm determined by alkyl chain length. In the cell membrane, amphiphiles with diverse headgroup chemistry, including pendant carbohydrates, are used to mediate interactions with other cells and the extracellular matrix. Our findings point to the possibility that similarly diverse headgroup chemistries could be installed in striped phases, either directly through Langmuir-Schaefer conversion, or through post-assembly modification using common coupling chemistries. Overall, this illustrates a new route for controlled molecular-scale clustering of complex ligands such as carbohydrates at interfaces.

Conflicts of interest

There are no conflicts to declare.

Acknowledgements

SAC acknowledges support through a DARPA Young Faculty Award, N66001-17-1-4046.

Notes and references

1. Claridge, S. A. Standing, Lying, and Sitting: Translating Building Principles of the Cell Membrane to Synthetic 2D Material Interfaces. *Chem. Commun.* **2018,** *54*, 6681-6691.
2. Love, J. C.; Estroff, L. A.; Kriebel, J. K.; Nuzzo, R. G.; Whitesides, G. M. Self-Assembled Monolayers of Thiolates on Metals as a Form of Nanotechnology. *Chem. Rev.* **2005,** *105*, 1103-1169.
3. Aizenberg, J.; Black, A. J.; Whitesides, G. M. Control of Crystal Nucleation by Patterned Self-Assembled Monolayers. *Nature* **1999,** *398*, 495-498.

4. Han, Y. J.; Aizenberg, J. Face-Selective Nucleation of Calcite on Self-Assembled Monolayers of Alkanethiols: Effect of the Parity of the Alkyl Chain. *Angew. Chem., Int. Ed.* **2003,** *42*, 3668-3670.
5. Pokroy, B.; Aizenberg, J. Calcite Shape Modulation through the Lattice Mismatch between the Self-Assembled Monolayer Template and the Nucleated Crystal Face. *CrystEngComm* **2007,** *9*, 1219-1225.
6. Liang, R.; Yan, L.; Loebach, J.; Ge, M.; Uozumi, Y.; Sekanina, K.; Horan, N.; Gildersleeve, J.; Thompson, C.; Smith, A.; Biswas, K.; Still, W. C.; Kahne, D. Parallel Synthesis and Screening of a Solid Phase Carbohydrate Library. *Science* **1996,** *274*, 1520-1522.
7. Oyelaran, O.; Gildersleeve, J. C. Glycan Arrays: Recent Advances and Future Challenges. *Curr. Opin. Chem. Biol.* **2009,** *13*, 406-413.
8. Kiessling, L. L.; Pohl, N. L. Strength in Numbers: Non-Natural Polyvalent Carbohydrate Derivatives. *Chem. Biol.* **1996,** *3*, 71-77.
9. Gestwicki, J. E.; Cairo, C. W.; Strong, L. E.; Oetjen, K. A.; Kiessling, L. L. Influencing Receptor-Ligand Binding Mechanisms with Multivalent Ligand Architecture. *J. Am. Chem. Soc.* **2002,** *124*, 14922-14933.
10. Kiessling, L. L.; Gestwicki, J. E.; Strong, L. E. Synthetic Multivalent Ligands as Probes of Signal Transduction. *Angew. Chem., Int. Ed.* **2006,** *45*, 2348-2368.
11. Kumar, A.; Whitesides, G. M. Features of Gold Having Micrometer to Centimeter Dimensions Can Be Formed through a Combination of Stamping with an Elastomeric Stamp and an Alkanethiol Ink Followed by Chemical Etching. *Appl. Phys. Lett.* **1993,** *63*, 2002-2004.
12. Kumar, A.; Biebuyck, H. A.; Whitesides, G. M. Patterning Self-Assembled Monolayers: Applications in Materials Science. *Langmuir* **1994,** *10*, 1498-1511.
13. Perl, A.; Reinhoudt, D. N.; Huskens, J. Microcontact Printing: Limitations and Achievements. *Adv. Mater.* **2009,** *21*, 2257-2268.
14. Xia, Y. N.; Whitesides, G. M. Soft Lithography. *Annu. Rev. Mater. Sci.* **1998,** *28*, 153-184.
15. Park, S.; Gildersleeve, J. C.; Blixt, O.; Shin, I. Carbohydrate Microarrays. *Chem. Soc. Rev.* **2013,** *42*, 4310-4326.
16. Kiessling, L. L. Chemistry-Driven Glycoscience. *Bioorg. Med. Chem.* **2018,** *26*, 5229-5238.
17. Han, X.; Zheng, Y.; Munro, C. J.; Ji, Y.; Braunschweig, A. B. Carbohydrate Nanotechnology: Hierarchical Assembly Using Nature's Other Information Carrying Biopolymers. *Curr. Opin. Biotechnol.* **2015,** *34*, 41-47.
18. Groszek, A. J. Preferential Adsorption of Normal Hydrocarbons on Cast Iron. *Nature* **1962,** *196*, 531-533.
19. Groszek, A. J. Preferential Adsorption of Long-Chain Normal Paraffins on MoS_2 WS_2 and Graphite from N-Heptane. *Nature* **1964,** *204*, 680.
20. Rabe, J. P.; Buchholz, S. Commensurability and Mobility in 2-Dimensional Molecular Patterns on Graphite. *Science* **1991,** *253*, 424-427.
21. Grim, P. C. M.; De Feyter, S.; Gesquiere, A.; Vanoppen, P.; Rucker, M.; Valiyaveettil, S.; Moessner, G.; Mullen, K.; De Schryver, F. C. Submolecularly Resolved Polymerization of Diacetylene Molecules on the Graphite Surface Observed with Scanning Tunneling Microscopy. *Angew. Chem., Int. Ed.* **1997,** *36*, 2601-2603.
22. Cyr, D. M.; Venkataraman, B.; Flynn, G. W. STM Investigations of Organic Molecules Physisorbed at the Liquid-Solid Interface. *Chem. Mater.* **1996,** *8*, 1600-1615.
23. Okawa, Y.; Aono, M. Linear Chain Polymerization Initiated by a Scanning Tunneling Microscope Tip at Designated Positions. *J. Chem. Phys.* **2001,** *115*, 2317-2322.
24. Okawa, Y.; Akai-Kasaya, M.; Kuwahara, Y.; Mandal, S. K.; Aono, M. Controlled Chain Polymerisation and Chemical Soldering for Single-Molecule Electronics. *Nanoscale* **2012,** *4*, 3013-3028.
25. Li, B.; Tahara, K.; Adisoejoso, J.; Vanderlinden, W.; Mali, K. S.; De Gendt, S.; Tobe, Y.; De Feyter, S. Self-Assembled Air-Stable Supramolecular Porous Networks on Graphene. *ACS Nano* **2013,** *7*, 10764-10772.
26. Bang, J. J.; Rupp, K. K.; Russell, S. R.; Choong, S. W.; Claridge, S. A. Sitting Phases of Polymerizable Amphiphiles for Controlled Functionalization of Layered Materials. *J. Am. Chem. Soc.* **2016,** *138*, 4448-4457.
27. Hayes, T. R.; Bang, J. J.; Davis, T. C.; Peterson, C. F.; McMillan, D. G.; Claridge, S. A. Multimicrometer Noncovalent Monolayer Domains on Layered Materials through Thermally Controlled Langmuir-Schaefer Conversion for Noncovalent 2D Functionalization. *ACS Appl. Mater. Interf.* **2017,** *9*, 36409–36416.
28. Villarreal, T. A.; Russell, S. R.; Bang, J. J.; Patterson, J. K.; Claridge, S. A. Modulating Wettability of Layered Materials by Controlling Ligand Polar Headgroup Dynamics. *J. Am. Chem. Soc.* **2017,** *139*, 11973-11979.
29. Davis, T. C.; Bang, J. J.; Brooks, J. T.; McMillan, D. G.; Claridge, S. A. Hierarchically Patterned Noncovalent Functionalization of 2D Materials by Controlled Langmuir-Schaefer Conversion. *Langmuir* **2018,** *34*, 1353-1362.
30. Bang, J. J.; Porter, A. G.; Davis, T. C.; Hayes, T. R.; Claridge, S. A. Spatially Controlled Noncovalent Functionalization of 2D Materials Based on Molecular Architecture *Langmuir* **2018,** *34*, 5454-5463.
31. Choong, S. W.; Russell, S. R.; Bang, J. J.; Patterson, J. K.; Claridge, S. A. Sitting Phase Monolayers of Polymerizable Phospholipids Create Dimensional, Molecular-Scale Wetting Control for Scalable Solution Based Patterning of Layered Materials. *ACS Appl. Mater. Interf.* **2017,** *9*, 19326-19334.
32. Porter, A. G.; Ouyang, T.; Hayes, T. R.; Biechele-Speziale, J.; Russell, S. R.; Claridge, S. A. 1-nm-Wide Hydrated Dipole Arrays Regulate AuNW Assembly on Striped Monolayers in Nonpolar Solvent. *In review* **2019**.
33. Workman, R. K.; Schmidt, A. M.; Manne, S. Detection of a Diffusive Two-Dimensional Gas of Amphiphiles by Lateral Force Microscopy. *Langmuir* **2003,** *19*, 3248-3253.
34. Workman, R. K.; Manne, S. Molecular Transfer and Transport in Noncovalent Microcontact Printing. *Langmuir* **2004,** *20*, 805-815.
35. Hovis, J. S.; Boxer, S. G. Patterning and Composition Arrays of Supported Lipid Bilayers by Microcontact Printing. *Langmuir* **2001,** *17*, 3400-3405.
36. Russell, S. R.; Davis, T. C.; Bang, J. J.; Claridge, S. A. Spectroscopic Metrics for Alkyl Chain Ordering in Lying-Down Noncovalent Monolayers of Diynoic Acids on Graphene. *Chem. Mater.* **2018,** *30*, 2506-2514.
37. Miura, A.; De Feyter, S.; Abdel-Mottaleb, M. M. S.; Gesquiere, A.; Grim, P. C. M.; Moessner, G.; Sieffert, M.; Klapper, M.; Mullen, K.; De Schryver, F. C. Light- and STM-Tip-Induced Formation of One-Dimensional and Two-Dimensional Organic Nanostructures. *Langmuir* **2003,** *19*, 6474-6482.
38. Giridharagopal, R.; Kelly, K. F. Substrate-Dependent Properties of Polydiacetylene Nanowires on Graphite and MoS_2. *ACS Nano* **2008,** *2*, 1571-1580.
39. Wang, Z.; Volinsky, A. A.; Gallant, N. D. Crosslinking Effect on Polydimethylsiloxane Elastic Modulus Measured by Custom-Built Compression Instrument. *J. Appl. Polym. Sci.* **2014,** *131*, 41050.
40. Xia, Y.; Whitesides, G. M. Use of Controlled Reactive Spreading of Liquid Alkanethiol on the Surface of Gold to Modify the Size of

Features Produced by Microcontact Printing. *J. Am. Chem. Soc.* **1995,** *117*, 3274-3275.

41. Sharpe, R. B. A.; Burdinski, D.; Huskens, J.; Zandvliet, H. J. W.; Reinhoudt, D. N.; Poelsema, B. Spreading of 16-Mercaptohexadecanoic Acid in Microcontact Printing. *Langmuir* **2004,** *20*, 8646-8651.

42. Libioulle, L.; Bietsch, A.; Schmid, H.; Michel, B.; Delamarche, E. Contact-Inking Stamps for Microcontact Printing of Alkanethiols on Gold. *Langmuir* **1999,** *15*, 300-304.

43. Graham, D. J.; Price, D. D.; Ratner, B. D. Solution Assembled and Microcontact Printed Monolayers of Dodecanethiol on Gold: A Multivariate Exploration of Chemistry and Contamination. *Langmuir* **2002,** *18*, 1518-1527.

44. Doudevski, I.; Hayes, W. A.; Schwartz, D. K. Submonolayer Island Nucleation and Growth Kinetics During Self-Assembled Monolayer Formation. *Phys. Rev. Lett.* **1998,** *81*, 4927-4930.

45. Sharpe, R. B. A.; Burdinski, D.; van der Marel, C.; Jansen, J. A. J.; Huskens, J.; Zandvliet, H. J. W.; Reinhoudt, D. N.; Poelsma, B. Ink Dependence of Poly(Dimethylsiloxane) Contamination in Microcontact Printing. *Langmuir* **2006,** *22*, 5945-5951.

46. Claridge, S. A.; Liao, W.-S.; Thomas, J. C.; Zhao, Y.; Cao, H. H.; Cheunkar, S.; Serino, A. C.; Andrews, A. M.; Weiss, P. S. From the Bottom Up: Dimensional Control and Characterization in Molecular Monolayers. *Chem. Soc. Rev.* **2013,** *42*, 2725-2745.

47. Srinivasan, C.; Mullen, T. J.; Hohman, J. N.; Anderson, M. E.; Dameron, A. A.; Andrews, A. M.; Dickey, E. C.; Horn, M. W.; Weiss, P. S. Scanning Electron Microscopy of Nanoscale Chemical Patterns. *ACS Nano* **2007,** *1*, 191-201.

48. Delamarche, E.; Schmid, H.; Bietsch, A.; Larsen, N. B.; Rothuizen, H.; Michel, B.; Biebuyck, H. Transport Mechanisms of Alkanethiols During Microcontact Printing on Gold. *J. Phys. Chem. B* **1998,** *102*, 3324-3334.

